ELSEVIER

Nuclear Medicine and Biology 30 (2003) 761–769

NUCLEAR MEDICINE — AND — BIOLOGY

www.elsevier.com/locate/nucmedbio

Radiolabeling of magnetic targeted carriers (MTC) with indium-111

Urs O. Häfeli[a,*], Junfeng Yu[b], Farhad Farudi[c], Yuhua Li[d], Gilles Tapolsky[d]

[a]*Cleveland Clinic Foundation, Department of Radiation Oncology, 9500 Euclid Ave T28, Cleveland, OH, 44195, USA*
[b]*Shanghai Institute of Nuclear Research, Chinese Academy of Sciences, 2019 Jialuo Road, Jiading, Shanghai 201800, P.R. China*
[c]*Cleveland Clinic Foundation, Department of Cardiology, 9500 Euclid Ave F25, Cleveland, OH 44195, USA*
[d]*FeRx Inc., 12635 E. Montview Blvd.-Suite 300, Aurora, CO 80010, USA*

Received 20 February 2003; received in revised form 20 April 2003; accepted 25 April 2003

Abstract

Magnetic targeted carriers (MTC) are magnetically susceptible microparticles that can be physically targeted to a specific site. MTC were radiolabeled with ^{111}In using three different methods. Reaction parameters were investigated in order to optimize the final properties of the labeled MTC. The reaction parameters studied were chelation agent, chelation time, temperature, radiolabeling time, solvent, and molar ratios. A 97.7 ± 0.9% binding efficiency and plasma stability of 92.6 ± 0.1% over 7 days were achieved when 2-p-aminobenzyl-1,4,7,10-tetraazacyclododecane-1,4,7,10-tetra-acetic acid (ABz-DOTA) was used as the chelating agent. A preliminary animal biodistribution study confirmed the binding stability. The labeling of the MTC with the diagnostic isotope ^{111}In was undertaken to allow for quantitative imaging and dosimetry prior to therapy with ^{90}Y radiolabeled MTC.

Keywords: Magnetic targeting; Microspheres; Radiolabeling; Indium-111; Yttrium-90; Imaging

1. Introduction

Radioactive microparticles of different chemical compositions are currently used for diagnostic or therapeutic applications [1]. The main issue related to the use of therapeutic radiopharmaceuticals is the biodistribution following administration and the resulting doses delivered to non-targeted organs and tissues. In some instance, these doses lead to organ specific toxicities, which would limit the amount of activity that can be administered, resulting in suboptimal treatment effects and decreased therapeutic benefit.

Different targeting mechanisms have been developed to circumvent suboptimal biodistribution and deliver pharmaceutical agents specifically to diseased cells or cancerous tumors [2–6]. A chemical targeting approach was proposed to target specific cell surface antigens using peptides or antibodies [7,8]. However, the biochemical differences between normal and cancerous cells are typically more quantitative than qualitative, leading to a lack of specificity for this biochemical recognition and to toxic side effects. Since the early experiments, new generations of more selective antibodies and peptides have been developed but further improvements are still needed to focus them into the target area. While several diagnostic and therapeutic radiolabeled products based on antibody or peptide targeting mechanisms are in the late stages of clinical development, Zevalin® has been recently approved by the Food and Drug Administration (FDA) to treat certain forms of non-Hodgkin's lymphoma [9]. This therapy is based on an ^{90}Y (yttrium-90) radiolabeled antibody, ibritumomab tiuxetan, and includes an initial imaging step based on the same antibody radiolabeled with ^{111}In (indium-111). The imaging step allows physicians to determine the actual patient pharmacokinetics, biodistribution, and organ dosimetry that could be anticipated with the therapeutic product. This step further permits for modification of the therapeutic dose when local toxicity is anticipated based on the imaging results [10].

Radioactive microspheres have been developed as another targeting approach to localize the activity to a specific organ. Recently, FDA approved microparticles containing ^{90}Y which are used either alone for primary liver tumors (Theraspheres©; [11]) or in combination with systemic administration of 5-fluorouracil for the treatment of colorectal cancer liver metastases (SIR-Spheres©; [12]). The mechanism of localization of these large microparticles to the liver

* Corresponding author. Tel.: +1-216-444-2174; Fax: +1-216-445-4480.
E-mail address: hafeliu@ccf.org (U.O. Hafeli).

0969-8051/03/$ – see front matter
doi:10.1016/S0969-8051(03)00077-5

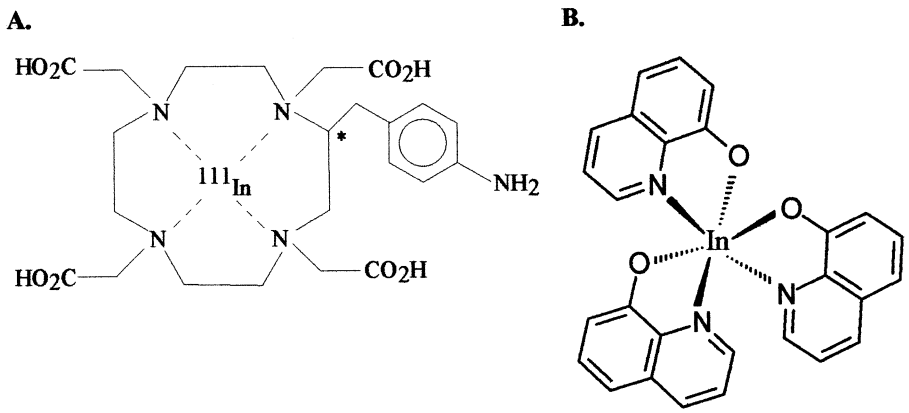

Fig. 1. Structure of chelated ^{111}In. A. ^{111}In-2-p-aminobenzyl-1,4,7,10-tetraazacyclododecane-1,4,7,10-tetra-(acetic acid) (^{111}In-ABz-DOTA). In ^{111}In-DOTA, the aminobenzyl-group is replaced by an H-atom; B. ^{111}In oxyquinoline (^{111}In-oxine).

is based on embolization of the tumor vasculature after their direct injection into the hepatic artery and is as such only of limited cancer selectivity.

Magnetic microspheres have been proposed and developed to improve targeting efficiency and selectively deliver pharmaceutical agents to cancerous cells, tumors, and organs [13]. Although the primary application of radioactive magnetic microspheres has been as a diagnostic tool to investigate the body distribution of magnetic drugs, therapeutic uses are currently being developed, especially for the treatment of cancer [14].

Magnetic targeted carriers (MTC) are being developed by FeRx Incorporated for the site specific delivery of pharmaceutical agents. These microparticles are composed of metallic iron and activated carbon and are prepared by a high-energy milling process [15]. MTC range in size from 0.5 μm to 5 μm with an average diameter of approximately 1.5 μm. The synergy between these two components creates a magnetically susceptible microparticle that may be targeted and localized at a specific site. At the same time, this microparticle is capable of carrying therapeutic quantities of a wide range of pharmaceutical agents [15]. MTC can also be labeled with therapeutic radioisotopes to treat chemoresistant tumors [16]. We recently labeled MTC with the therapeutic radioisotope ^{188}Re (rhenium-188) [17]. The labeling efficiency was higher than 95% and the serum stability satisfactory. However, due to the limited availability of ^{188}W/^{188}Re-generators [18–20], other commercially available radionuclides were studied. Among these, the β-emitter ^{90}Y and its diagnostic γ-emitting analog ^{111}In are preferred since they have been used for many years in nuclear pharmacies to prepare diagnostic and therapeutic radiopharmaceuticals.

The aim of this paper is to report the optimal conditions for the radiolabeling of MTC with ^{111}In and test the in vivo stability of the radiolabeled complex. Three labeling methods were used. First, $^{111}InCl_3$ was directly incubated with the MTC. Second, the chelator 1,4,7,10-tetraazacyclododecane-1,4,7,10-tetra(acetic acid) (DOTA) and a derivative thereof were used to chelate ^{111}In and then adsorb this radioactive compound onto the MTC. Finally, ^{111}In-oxine was adsorbed onto the MTC. Reaction parameters were studied in order to improve and compare the properties of the final products and the most stable radioactive MTC were then tested in vivo.

2. Methods

2.1. Preparation of chelated ^{111}In-compounds

The chelation of ^{111}In (PerkinElmer Life Sciences, Boston, MA), was performed using 1,4,7,10-tetraazacyclododecane-1,4,7,10-tetra-(acetic acid) (DOTA), 2-p-aminobenzyl-DOTA (ABz-DOTA) (Macrocyclics, Dallas, TX) (Figure 1A), or oxine (= 8-hydroxyquinoline; Sigma-Aldrich, St. Louis, MO) (Figure 1B).

Several parameters for the chelation reaction were investigated. The reaction was performed by incubating different molar ratios (MRs) of DOTA or ABz-DOTA to ^{111}In (from 50:1 to 10^5:1) in 0.2 M or 0.02 M ammonium acetate buffer at pH 6 for 0 to 40 minutes at temperatures from 22 to 90 °C in an Eppendorf Thermomixer (Brinkmann Instruments, Inc., Germany) at 1400 rpm. The chelation efficiency was investigated as a function of indium concentration ranging from 1 to 5 μM. When using oxine as a chelator, 10 μCi of ^{111}In in 200 μl of 0.2 M or 0.02 M ammonium acetate buffer at pH 6 was incubated with 200 μl of a 0.1 M oxine solution in ethanol for 15 min at 50 °C. ^{111}In-oxine was then extracted twice with 200 μl CH_2Cl_2.

Chelation efficiencies of ^{111}In-DOTA and ^{111}In-ABz-DOTA were determined using thin layer chromatography (TLC) using silica precoated strips (Polygram Sil G/UV_{254}) as the solid phase and a mixture of 80% NH_4Ac 10% and 20% methanol as the mobile phase (Table 1). Free $^{111}In^{3+}$ migrates with the solvent front (R_f 0.7–1.0) and ^{111}In-MTC or ^{111}In colloids stay at the origin (R_f 0). The R_f of ^{111}In-DOTA or ^{111}In-ABz-DOTA is 0.2-0.5. This method was

Table 1
TLC systems for the analysis of ^{111}In, ^{111}In-DOTA and ^{111}In-ABz-DOTA

Stationary phase	Solvent	R_f Values			Comments
		Free $^{111}In^{3+}$	^{111}In-DOTA	^{111}In-ABz-DOTA	
Sil G/UV_{254}*	10% NH_4Ac (pH 4): methanol = 8:2	0.7–1.0	0.2–0.5	0.2–0.5	3-5 min development; ^{111}In-MTC with R_f 0
Whatman 3 mm[1]	Methanol	0–0.1	0.1–0.2		Overlap
	10% NH_4Ac (pH 4)	0.8–1	0.8–1		Overlap
Tec-Strip[2]	10% NH_4Ac (pH 4): methanol = 1:1	0.8–1	0.6–0.8		Overlap
	10% NH_4Ac (pH 4): methanol = 5:95	0–0.3		0.3–0.8	Overlap
	Ethanol or isopropanol	0	0–0.6	0–0.6	Overlap
	Methanol: HAc = 95:5 or 99:1	1		0.0–1.0	One peak
	10% NH_4Ac (pH 4)	0.8–1		0.6–0.8	Overlap
	Methanol	0		0.6–0.8	
ITLC[3]	Methanol	0	0.5–0.7	0.6–0.8	1–2 min development
Whatman 17[4]	Water	0		0.8–1	Two nice peaks

* Polygram® Sil G/UV_{254}, pre-coated sheets.
[1] Whatman 3 mm chromatography paper, Cat No. 3030917.
[2] Tec-Control™, black strips. #151-005 (Biodex Medical Systems).
[3] Gelman Sciences, silica gel impregnated glass fiber sheets, Instant Thin Layer Chromatography, Prod. 61886.
[4] Whatman 17 chromatography paper, Lot No. 3017915.

found to be optimal for use with a radiation scanner (Figure 2). Other TLC methods investigated are also described in Table 1 and might be useful if the TLCs were to be cut and analyzed in a γ-counter (Figure 3).

The TLC method for the analysis of the chelation efficiency of ^{111}In-oxine consisted of Tec-Control strips (Biodex Medical Systems) as the stationary phase and methanol as the mobile phase. In this system, ^{111}In-oxine migrates with the solvent front (R_f = 0.8–1.0) while free ^{111}In stays at the origin (R_f = 0).

2.2. Adsorption of ^{111}In-compounds to MTC and stability measurement

The direct adsorption of the positively charged $^{111}In^{3+}$ on the MTC was investigated first. Twenty milligram of MTC were incubated for 30 min at 37 °C with 100 μl of $^{111}InCl_3$ (~100 μCi) in 0.2 M NH_4Ac buffer at pH 6 in an Eppendorf Thermomixer at 1400 rpm. The radiolabeled MTC were then washed twice with PBS pH 7.4.

The ^{111}In-labeled DOTA-complex was adsorbed onto the MTC after assessment of the chelation efficiency. Typically, 20 mg of MTC were incubated with 100 μl or 200 μl of a solution containing 30 to 140 μCi of the chelated radioisotope for 30 to 90 min and at temperatures between 37 and 90°C. For ^{111}In-oxine, 100 μl of the methylene chloride solution was transferred to 20 mg of MTC and incubated at 60°C for 30 min until complete evaporation of the solvent.

The binding efficiency, or amount of activity effectively adsorbed onto the MTC microparticles for the two methods described above was then determined by bringing the vol-

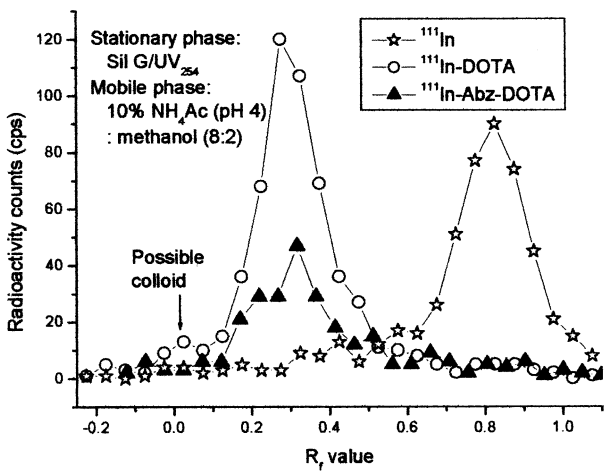

Fig. 2. TLC system for analysis of ^{111}In-DOTA and ^{111}In-ABz-DOTA using a radiation scanner.

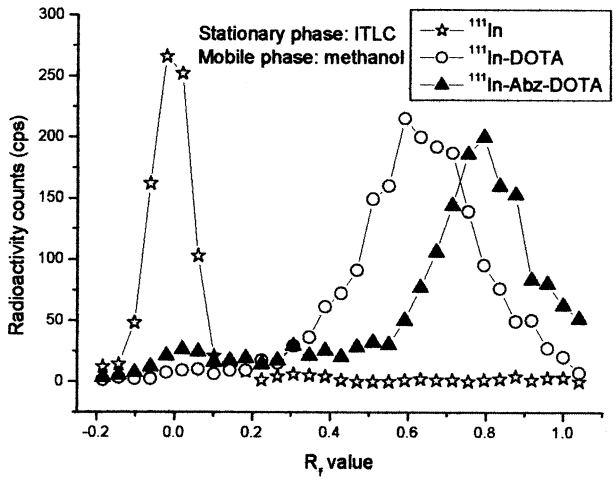

Fig. 3. TLC system for analysis of ^{111}In-DOTA and ^{111}In-ABz-DOTA in the γ-counter.

ume of the ^{111}In-labeled MTC suspension up to 1 ml with PBS (pH 7.4) and measuring the total radioactivity in a RadCal dose calibrator using a setting for ^{111}In with a calibration factor of 1141 (Radcal Corp., Monrovia, CA). After centrifugation, the supernatant was removed and 1 ml fresh PBS added (wash 1). The suspension was centrifuged and the supernatant removed, then 1.5 ml of human plasma or viscous vehicle was added and the total activity counted (radioactivity after wash 2).

$$\text{MTC binding efficiency [\%]} = \frac{\text{Radioactivity after 2 washes}}{\text{Total radioactivity before washes}} \times 100\%$$

The in vitro stability of the adsorption of free or chelated indium onto the MTC was investigated in a viscous aqueous solution of 0.5% sodium carboxymethylcellulose and 10% mannitol which is used for the in vivo administration of the MTC, and also in human plasma at 37°C. At each time point (1 hour, 1, 3, and 7 days), the sample with the ^{111}In-labeled MTC was removed from the 37°C water bath and the total radioactivity measured. The vial was then centrifuged and two 500 μl aliquots of supernatant (from a total of 1500 μl) were removed and transferred to clean vials. Activities of the two vials of supernatant were measured using a γ-counter (HP Minaxi Autogamma 5000 counter). The volume of plasma taken from the samples was replaced by adding 1 ml of fresh plasma to the sample vial. Stability measurements as a function of time were made by calculating the ratio of the activity in solution (released from the MTC) to the total activity measured for the suspension:

$$\text{MTC bound [\%]} = 1 - \frac{\text{Average radioactivity of 500 } \mu\text{l supernatant} \times 3}{\text{Total radioactivity}} \times 100\%$$

2.3. Animal experiment

We evaluated the in vivo stability of the bound activity and the biodistribution of radioactivity in Wistar rats following intramuscular administration. The experiment was performed according to the guidelines for the Care and Use of Laboratory Animals published by NIH, using a protocol approved by the Cleveland Clinic Foundation's animal review committee. Twelve female Wistar rats (200-250 g) were divided into 2 groups. The radioactive ^{111}In-ABz-DOTA was prepared by diluting 5 μl of ^{111}In in 0.05 M HCl (2 mCi) with 170 μl of 0.02 M ammonium acetate buffer pH 6 and 30 μl of 1 mM ABz-DOTA, and then incubating for 30 minutes at 90°C. The labeling efficiency was 97.4%. For the control group, 100 μl of the solution was diluted with 1.5 ml of the viscous injection solution. For the experimental group MTC were radiolabeled with ^{111}In-ABz-DOTA by adding 100 μl of the ^{111}In-ABz-DOTA solution to 16 mg of MTC, incubating under stirring for 30 minutes at 90°C, and then diluting with 1.5 ml of the viscous injection solution. All animals received 200 μl of the ^{111}In-labeled compound (70 μCi) injected into the left thigh muscle. Two rats of each group were sacrificed 3, 24, and 72 hours after injection. The total radioactivity for each animal was measured in the Radcal dose calibrator before dissection, and the total activity remaining in the carcass after dissection was also measured. Blood samples and organs were weighed and the radioactivity measured in a γ-counter. The organ activity in percent of total injected activity (%ID) was calculated by dividing the organ radioactivity by the sum of all organ radioactivity plus the radioactivity left in the carcass. The organ/blood ratio was calculated by dividing each organ's radioactivity concentration (Bq/mg) by the radioactivity concentration measured in blood at each time point.

3. Results and discussion

The main characteristics of radiolabeled MTC we wanted to optimize were the binding efficiency, as determined by the effectiveness of the adsorption of the radioisotope onto the MTC, and the stability of this adsorption over time. Studies were performed in order to identify the parameters influencing these properties and find the conditions for optimal results. Similarly, the parameters of the chelation step were studied in order to reproducibly obtain the highest possible yield.

3.1. Preparation of the chelated ^{111}In-compounds

Radioactive complexes are often made by chelation, a reversible process with defined association constants (K_m) [21]. Reaction parameters can influence the equilibrium and thus the formation and stability of the complex. It has been shown by several investigators that the ratio of chelating species to radioisotope needs to be carefully controlled for optimal binding and stability [22,23]. In our studies, the mole ratio (MR) is defined as:

$$\text{Mole ratio (MR)} = \frac{\text{Mole of chelator}}{\text{Mole of indium } (In)}$$

If the ratio is too low, leading to an excess of indium, the chelation will be incomplete, allowing unchelated indium to bind to the surface of vials and containers or react with contaminants, thus possibly leading to a large loss of radioactivity. If the ratio is too high, resulting in an excess of chelator, it might affect the adsorption properties onto the MTC, as well as the long-term stability of the chelated indium adsorbed onto the MTC. In order to have the highest binding efficiency and optimal stability, we investigated different MRs of the chelators, DOTA and ABz-DOTA, to indium. These compounds were chosen because the planar

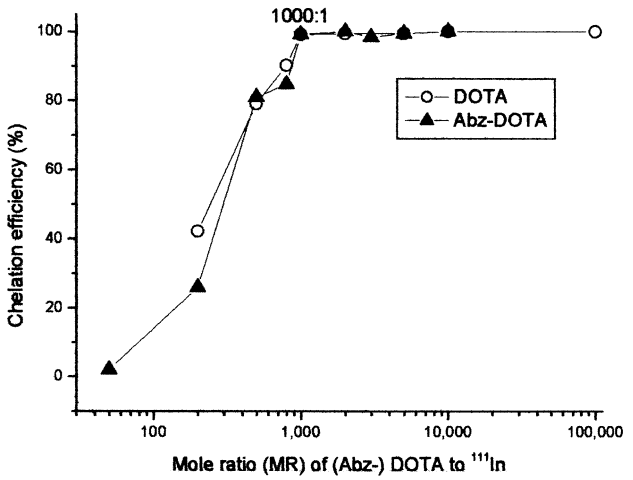

Fig. 4. Effect of DOTA (ABz-DOTA)/^{111}In mole ratio (MR) on chelation efficiency at an indium concentration of 0.01 μM (n=1).

ligand DOTA [24] shows good biodistribution and toxicity properties [25–27] and is reported to be the most stable chelator of ^{90}Y for clinical applications [28,29]. The additional amino-benzyl group in ABz-DOTA may alter the kinetics, or the extent and stability of adsorption to the MTC, and therefore could be beneficial for keeping the radioactive compound adsorbed onto the MTC for extended periods of time. The chelation reaction does not seem to be influenced by the molarity of the buffer. Ammonium acetate buffers of 0.2 M or 0.02 M gave identical chelation efficiencies of chelated ^{111}In (data not shown). At the low indium concentration of 0.01 μM, high MRs of about 1000:1 are necessary to reach high chelation efficiency (Figure 4). Lengthening the incubation times to more than 20 minutes did not improve the chelation efficiencies (Figure 5). To investigate the optimal indium concentration for reliable and reproducible chelation, we increased the indium concentration up to 5 μM by adding the non-radioactive carrier indium trichloride (Figure 6). At an indium concentration of 3 μM, an MR of 50:1 for DOTA was needed to reach a chelation efficiency of 95.1 ± 2.5% (n = 5) (Figure 6). For ABz-DOTA at an indium concentration of 3 μM and MR of 50:1, a chelation efficiency of 96.9% ± 2.2% was measured (n = 5). Further increasing the indium concentrations to the maximum tested of 4 or 5 μM, or increasing the MR, did not improve the chelation efficiency. The optimal indium concentration determined for both DOTA and ABz-DOTA was 3 μM in the ammonium acetate buffer. The effect of the temperature on the chelation efficiency was investigated at 0.01 μM indium with a MR of 1000:1, using a heating time of 20 min. The maximum tested temperature of 90 °C showed the highest chelation efficiency (Figure 7). For this reason, and because longer incubation times did not increase the chelation efficiency (Figure 5), we performed our chelation step at 90 °C for 30 min.

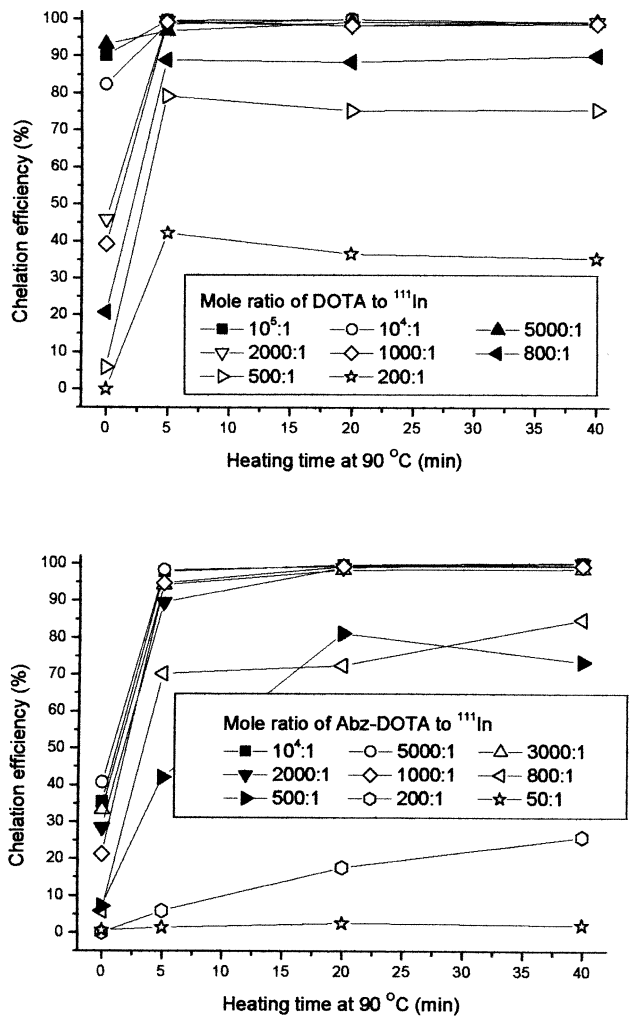

Fig. 5. Influence of incubation time and MR at 90 °C on chelation efficiency (n=1).

3.2. Direct binding of ^{111}In onto MTC

The direct binding of ^{111}In onto the MTC led to a low binding efficiency of 83.7 ± 1.2%. Stability tests showed that only 61.5 ± 4.0% of the radioactivity initially bound to the MTC remained onto the MTC after a week in human plasma at 37 °C (Figure 8). Directly adsorbing ^{111}In to MTC thus does not produce a stable product and does not appear appropriate for potential in vivo applications.

3.3. Adsorption and stability of chelated ^{111}In-compounds to MTC

Optimal reaction parameters for the adsorption of ^{111}In-ABz-DOTA onto MTC were reached with a 30 min incubation time at 90 °C. The binding efficiency was 97.7 ± 0.9%. For this binding step with the ABz-DOTA chelator, neither the incubation volume nor the temperature were critical. Incubating the MTC in 100 and 200 μl at 50 °C resulted in a binding efficiency of 94.7 ± 0.1% and 93.7 ±

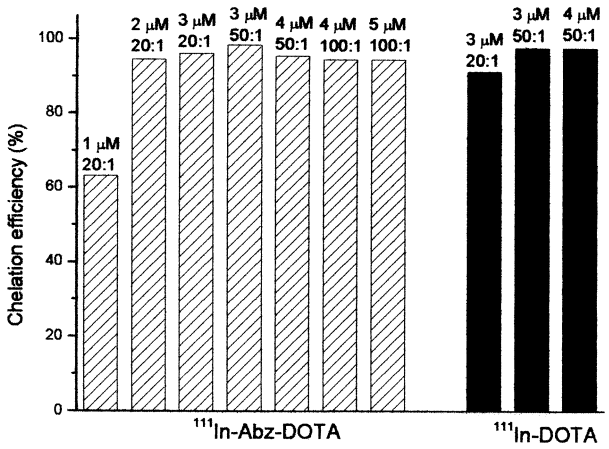

Fig. 6. Effect of indium concentration and MR on chelation efficiency (n=1).

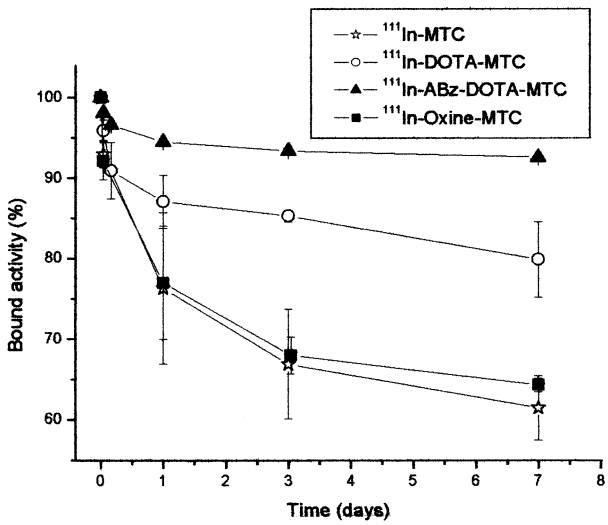

Fig. 8. Binding stability of ^{111}In-MTC, ^{111}In-DOTA-MTC, ^{111}In-ABz-DOTA-MTC, and ^{111}In-oxine in human plasma at 37 °C (n=3).

0.4%, respectively. Changing the temperature between 37°C and 90°C, for a 100 μl volume, only changed the binding efficiency by a few percent as seen in Figure 9.

The chemical nature of the chelator also influenced adsorption and stability of the radioactive complex significantly. When ^{111}In-DOTA was adsorbed onto the MTC in conditions comparable to that of ^{111}In-ABz-DOTA, the binding efficiency was only 84.9 ± 2.6%, compared to 96.9% ± 2.2% for ^{111}In-ABz-DOTA. In addition, the binding stability in plasma showed that MTC radiolabeled with ^{111}In-DOTA were not as stable as MTC radiolabeled with ^{111}In-ABz-DOTA as the activity still bound to the particles after 7 days at 37 °C was approximately 80% and 95%, respectively (Figure 8).

The lipophilic ^{111}In-oxine complex forms quickly and completely with a chelation efficiency of 99.5% ± 0.7. Due to the aromatic rings, the binding efficiency of ^{111}In-oxine compound onto the MTC was excellent as expected; after two PBS washes, the activity bound was 100% ± 2.5% (n=3). However, the radioactivity was slowly released from the MTC, with only 64.3 ± 0.8% of the radioactivity left on the MTC after 7 days in plasma (Figure 8). The slow release of the activity is believed to be linked to the chemical instability of the In-oxine complex [30] and not to the release of the intact complex, resulting in free ^{111}In as detected by TLC (not shown).

3.4. Biodistribution of ^{111}In-ABz-DOTA and ^{111}In-ABz-DOTA-MTC in rats

The in vivo stability of the radioactive MTC compounds was assessed by comparing the biodistribution of the chelated compounds alone and bound to the MTC. The choice of the intramuscular injection was made to more easily differentiate between activity in the form of the chelated

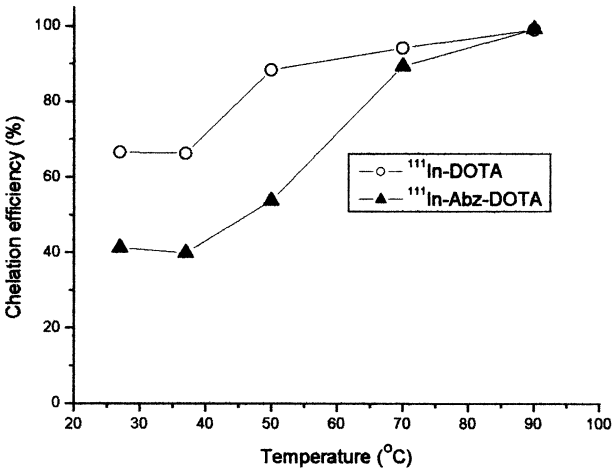

Fig. 7. Effect of temperature on chelation efficiency at a constant incubation time of 20 min (n=1).

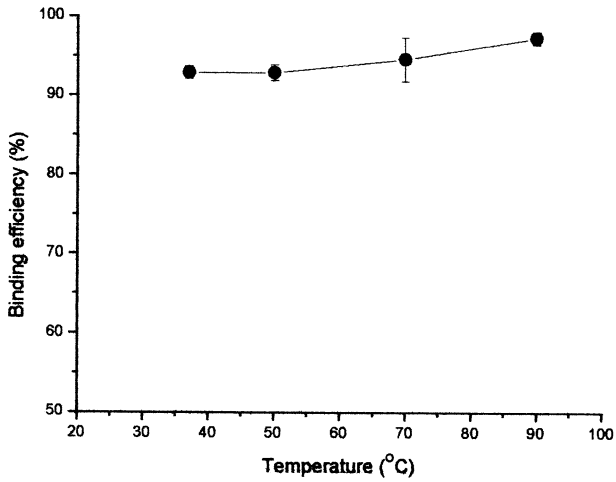

Fig. 9. Effect of temperature on MTC binding efficiency using ^{111}In-ABz-DOTA (n=3).

Table 2
Biodistribution of free and MTC-bound ^{111}In-ABz-DOTA in rats after intramuscular injection into the left thigh expressed as a percentage of the total injection activity (%ID) ± standard error (n = 2). It was calculated from the radioactivity concentration of each organ multiplied by the total organ weight and divided by the total activity in the rat at the time of sacrifice

Organ	Time point after injection					
	3 hours		1 day		3 days	
	^{111} In-ABz-DOTA	^{111}In-Abz-DOTA-MTC*	^{111}In-ABz-DOTA	^{111}In-ABz-DOTA-MTC	^{111}In-ABz-DOTA	^{111}In-ABz-DOTA-MTC
Blood	9.64 ± 1.91	0.87	5.54 ± 2.55	0.43 ± 0.25	2.21 ± 0.41	0.18 ± 0.10
Brain	0.06 ± 0.02	0.00	0.03 ± 0.02	0.01 ± 0.01	0.14 ± 0.03	0.01 ± 0.00
Thyroids	0.07 ± 0.02	0.00	0.15 ± 0.05	0.01 ± 0.00	0.20 ± 0.00	0.01 ± 0.00
Heart	0.15 ± 0.03	0.01	0.22 ± 0.01	0.01 ± 0.01	0.16 ± 0.00	0.01 ± 0.01
Lung	0.56 ± 0.13	0.03	0.56 ± 0.30	0.05 ± 0.02	0.60 ± 0.03	0.04 ± 0.02
Small intestine	3.97 ± 0.51	0.08	3.76 ± 1.12	0.09 ± 0.03	2.72 ± 0.19	0.20 ± 0.11
Stomach	0.37 ± 0.07	0.01	0.45 ± 0.17	0.02 ± 0.00	0.33 ± 0.04	0.02 ± 0.01
Spleen	0.17 ± 0.05	0.01	0.61 ± 0.08	0.03 ± 0.01	0.85 ± 0.07	0.04 ± 0.02
L. Kidney	3.16 ± 1.02	0.07	6.02 ± 0.86	0.13 ± 0.06	5.84 ± 0.12	0.17 ± 0.09
R. Kidney	3.80 ± 1.61	0.08	5.97 ± 0.72	0.13 ± 0.06	6.54 ± 0.04	0.17 ± 0.09
Liver	6.04 ± 1.10	0.21	9.10 ± 1.29	0.54 ± 0.26	15.32 ± 1.60	0.77 ± 0.45
L. Femur	0.11 ± 0.07	0.03	0.17 ± 0.09	0.08 ± 0.04	0.41 ± 0.19	0.03 ± 0.03
R. Femur	0.09 ± 0.01	0.00	0.16 ± 0.09	0.01 ± 0.01	0.20 ± 0.01	0.02 ± 0.01
Pancreas	0.15 ± 0.03	0.01	0.20 ± 0.03	0.01 ± 0.01	0.22 ± 0.05	0.02 ± 0.01
L. Thigh (Inj.)	3.71 ± 1.57	93.74	3.27 ± 0.73	92.92 ± 0.16	0.75 ± 0.60	94.77 ± 1.95
R. Thigh	0.10 ± 0.07	0.01	0.03 ± 0.00	0.01 ± 0.00	0.22 ± 0.07	0.01 ± 0.01
Pituitary gland	0.01 ± 0.00	0.00	0.00 ± 0.00	0.00 ± 0.00	0.00 ± 0.00	0.00 ± 0.00
Carcass**	67.83 ± 8.05	4.84	63.76 ± 0.79	5.53 ± 0.85	63.29 ± 1.14	3.52 ± 0.98

* Data of only one animal was used because of sample contamination. **Including 60% of blood.

indium and MTC-bound chelated indium. MTC do not redistribute after intramuscular injection (data not shown), thus the activity measured in different organs is linked to the release of the chelated indium from the MTC and subsequent organ redistribution.

The biodistribution of ^{111}In-ABz-DOTA and ^{111}In-ABz-DOTA-MTC following intramuscular injection in rat thighs differs significantly (Table 2). For ^{111}In-ABz-DOTA, the radioactivity quickly redistributes to the whole body. After 3 hours, more than 75% of the total injected activity had already cleared the system by urinary excretion. From the activity left in the animal's body at that time point, less than 4% of the radioactivity was found at the injection site, clearing at about the same rate as from the other organs thereafter. The small amount of radioactivity still found after 3 days was concentrated in the blood and the excreting organs (liver, kidney and small intestine).

In contrast, when the chelated complex was bound onto the MTC, no activity redistribution took place and approximately 93–94% of the activity was found at the site of injection at all time points measured in the study. In addition, the radioactivity measured in blood was less than 1% of the injected activity 3 hours after administration and decreased over the 3 days of the study. This indicates that only a small amount of the ^{111}In-compound is washed off the MTC under these conditions. Thus, the in vivo binding stability of the radiolabeled ^{111}In-ABz-DOTA-MTC seems satisfactory and correlates well with the in vitro results.

The significant differences between the biodistribution of the chelated indium and MTC-bound chelated indium are more apparent when comparing the organ-to-blood activities for each time point (Table 3). This comparison clearly shows that the complex ^{111}In-ABz-DOTA is rapidly cleared from the injection site through the blood supply. The only organs showing high levels of radioactivity are the excreting organs kidney, liver and spleen. The thigh-muscle:blood ratio was close to 5:1 (the thigh was the injection site) three hours after the injection of ^{111}In-ABz-DOTA while this ratio was on the order of 467:1 for ^{111}In-ABz-DOTA-MTC. Differences were even more pronounced over time, increasing from 1347:1 after 1 day to 3297:1 after 3 days, suggesting no redistribution from the site of injection.

4. Conclusions

Optimal conditions for the preparation of MTC radiolabeling with indium complexes were determined in this study. Of the 3 different methods investigated, the absorption of the hydrophilic radiolabeled complex ^{111}In-ABz-DOTA lead to the best labeling and stability results. The procedure to radiolabel MTC with ^{111}In is a simple two step procedure: chelation of the indium with ABz-DOTA followed by binding of the chelated indium to the MTC. These steps can be readily performed in a radiopharmacy. Yields for each step are excellent with chelation efficiencies on the order of 96-98% and binding efficiencies on the order of 95–97%. The in vitro binding stability of the complex ^{111}In-ABz-DOTA-MTC is satisfactory in plasma with approximately 93% of the radioactive complex still bound to

Table 3
Biodistribution of free and MTC-bound ^{111}In-ABz-DOTA in rats after intramuscular injection into the left thigh, expressed as organ/blood ratio ± standard error (n = 2). It was calculated from the radioactivity concentration of each organ (cpm/mg) divided by the radioactivity concentration of blood at each time point

Organ	Time point after injection					
	3 hours		1 day		3 days	
	^{111} In-ABz-DOTA	^{111}In-Abz-DOTA-MTC*	^{111}In-ABz-DOTA	^{111}In-ABz-DOTA-MTC	^{111}In-ABz-DOTA	^{111}In-ABz-DOTA-MTC
Blood	1.00 ± 0.00	1.00	1.00 ± 0.00	1.00 ± 0.00	1.00 ± 0.00	1.00 ± 0.00
Brain	0.07 ± 0.01	0.03	0.07 ± 0.00	0.12 ± 0.06	0.74 ± 0.24	0.46 ± 0.14
Thyroids	0.30 ± 0.01	0.10	1.33 ± 0.75	0.44 ± 0.01	3.23 ± 0.65	2.69 ± 0.04
Heart	0.37 ± 0.00	0.30	1.06 ± 0.53	0.56 ± 0.10	1.57 ± 0.21	1.20 ± 0.03
Lung	0.82 ± 0.05	0.54	1.04 ± 0.20	1.37 ± 0.45	3.13 ± 0.52	1.89 ± 0.04
Small intestine	0.85 ± 0.09	0.21	2.11 ± 1.42	0.68 ± 0.13	2.00 ± 0.74	1.54 ± 0.22
Stomach	0.48 ± 0.05	0.17	1.17 ± 0.11	1.03 ± 0.45	2.44 ± 0.68	1.72 ± 0.12
Spleen	0.48 ± 0.02	0.15	3.60 ± 1.71	1.75 ± 0.44	9.95 ± 1.42	7.20 ± 0.09
L. Kidney	5.34 ± 1.25	1.43	24.73 ± 13.07	5.52 ± 1.27	50.17 ± 5.12	16.87 ± 1.57
R. Kidney	5.94 ± 1.38	1.47	25.11 ± 19.66	5.28 ± 1.29	51.51 ± 11.41	15.68 ± 1.40
Liver	1.12 ± 0.01	0.47	3.05 ± 0.82	1.92 ± 0.27	10.54 ± 1.10	6.47 ± 0.38
L. Femur	1.06 ± 0.48	0.92	2.80 ± 1.69	9.68 ± 7.92	7.58 ± 2.17	5.25 ± 1.57
R. Femur	0.53 ± 0.09	0.25	2.26 ± 1.03	1.64 ± 0.80	4.65 ± 0.39	4.80 ± 0.19
Pancreas	0.39 ± 0.05	0.21	1.52 ± 0.75	0.99 ± 0.28	3.17 ± 0.49	3.12 ± 0.31
L. Thigh (Inj.)	4.97 ± 2.01	467	5.39 ± 2.69	1347 ± 779	9.86 ± 7.36	3297 ± 1492
R. Thigh	0.27 ± 0.06	0.24	0.69 ± 0.42	0.30 ± 0.02	1.58 ± 0.18	1.06 ± 0.03
Pituitary gland	0.53 ± 0.40	0.00	0.75 ± 0.67	1.14 ± 1.14	0.00 ± 0.00	0.06 ± 0.06

* Data of only one animal was used because of sample contamination.

the MTC after 7 days. The in vivo binding stability was confirmed following intramuscular injection. When comparing the chelated indium alone and the radiolabeled MTC, there was no release of the chelated indium from the MTC and no redistribution of the ^{111}In-ABz-DOTA-MTC microparticles as approximately 93% of the injected activity remains at the injection site 3 days after administration. These results indicate that the imaging characteristics of indium labeled MTC warrants further investigation as a diagnostic assessment tool prior to a therapeutic treatment based on ^{90}Y labeled MTC to determine the intra-patient biodistribution and organ dosimetry.

Acknowledgments

We thank FeRx Inc. (San Diego, CA) for supporting this work.

References

[1] Ercan MT. Radioactive microparticles. Part 2: Medical applications. In: Arshady R, editor. Microspheres, microcapsules and liposomes. Vol. 2. Citus Books: London, 1999. p. 313–42.
[2] Mayer LD. Future developments in the selectivity of anticancer agents: drug delivery and molecular target strategies. Cancer Metastasis Rev 1998;17:211–8.
[3] Dubowchik GM, Walker MA. Receptor-mediated and enzyme-dependent targeting of cytotoxic anticancer drugs. Pharmacol Therapeut 1999;83:67–123.
[4] Galanis E, Vile R, Russell SJ. Delivery systems intended for in vivo gene therapy of cancer: targeting and replication competent viral vectors. Crit Rev Oncol-Hematol 2001;38:177–92.
[5] Molema G. Tumor vasculature directed drug targeting: applying new technologies and knowledge to the development of clinically relevant therapies. Pharm Res 2002;19:1251–8.
[6] Luo Y, Prestwich GD. Cancer-targeted polymeric drugs. Curr Cancer Drug Targets 2002;2:209–26.
[7] Goldenberg DM. Targeted therapy of cancer with radiolabeled antibodies. J Nucl Med 2002;43:693–713.
[8] Heppeler A, Froidevaux S, Eberle AN, Maecke HR. Receptor targeting for tumor localisation and therapy with radiopeptides. Curr Med Chem 2000;7:971–94.
[9] Gordon LI, Witzig TE, Wiseman GA, et al. Yttrium 90 ibritumomab tiuxetan radioimmunotherapy for relapsed or refractory low-grade non-Hodgkin's lymphoma. Semin Oncol 2002;29:87–92.
[10] Wiseman GA, White CA, Stabin M, et al. Phase I/II ^{90}Y-Zevalin (yttrium-90 ibritumomab tiuxetan, IDEC-Y2B8) radioimmunotherapy dosimetry results in relapsed or refractory non-Hodgkin's lymphoma. Eur J Nucl Med 2000;27:766–77.
[11] Dancey JE, Shepherd FA, Paul K, et al. Treatment of nonresectable hepatocellular carcinoma with intrahepatic Y-90 microspheres. J Nucl Med 2000;41:1673–81.
[12] Gray B, Van Hazel G, Hope M, et al. Randomised trial of SIR-Spheres plus chemotherapy vs. chemotherapy alone for treating patients with liver metastases from primary large bowel cancer. Ann Oncol 2001;12:1711–20.
[13] Arshady R. Microspheres, Microcapsules & Liposomes: Magneto- and Radiopharmaceuticals. 3 vol. 1st ed. London: Citus Books, 2001.
[14] Häfeli UO. Chapter 18: Radiolabeled magnetic microcapsules for magnetically targeted radionuclide therapy. In: Arshady R, editor. Microspheres, Microcapsules & Liposomes: Radiolabeled and magnetic particulates in medicine and biology. Vol. 3. London: Citus Books, 2001. p. 559–84.
[15] Rudge SR, Kurtz TL, Vessely CR, Catterall LG, Williamson DL. Preparation, characterization, and performance of magnetic iron-carbon composite microparticles for chemotherapy. Biomat 2000;21:1411–20.

[16] Valentini V, Balducci M, Tortoreto F, Morganti AG, De Giorgi U, Fiorentini G. Intraoperative radiotherapy: current thinking. Eur J Surg Oncol 2002;28:180–5.
[17] Häfeli U, Pauer G, Failing S, Tapolsky G. Radiolabeling of magnetic particles with rhenium-188 for cancer therapy. J Mag Mag Mater 2001;225:73–8.
[18] Hayes RL, Rafter JJ. Rhenium-188 as possible diagnostic agent. J Nucl Med 1966;7:797.
[19] Callahan AP, Rice DE, Knapp FF. Availability of Rhenium-188 from a $^{188}W/^{188}Re$ Generator system for therapeutic applications. J Nucl Med 1987;28:656–7.
[20] Knapp FF. Rhenium-188-A generator derived radioisotope for cancer therapy. Cancer Biother Radiopharm 1998;13:337–49.
[21] Clarke ET, Martell AE. Stabilities of trivalent metal ion complexes of the tetraacetate derivatives of 12-, 13, and 14-membered tetraaza-macrocycles. Inorganica Chimica Acta 1991;190:37–46.
[22] Li M, Meares CF, Zhong GR, Miers L, Xiong CY, DeNardo SJ. Labeling monoclonal antibodies with ^{90}Yttrium- and ^{111}Indium-DOTA chelates: A simple and efficient method. Biocon Chem 1994; 5:101–4.
[23] DeNardo SJ, Zhong GR, Salako Q, Li M, DeNardo GL, Meares CF. Pharmacokinetics of chimeric L6 conjugated to Indium-111 and Yttrium-90-DOTA-peptide in tumor bearing mice. J Nucl Med 1995; 36:829–36.
[24] Moi MK, Meares CF, DeNardo SJ. The peptide way to macrocyclic bifunctional chelating agents: Synthesis of p-nitrobenzyl-DOTA and study of its yttrium(III) complex. J Am Chem Soc 1988;110:6266–7.
[25] Allard M, Doucet D, Kien P, Bonnemain B, Caille JM. Experimental study of DOTA-gadolinium. Pharmacokinetics and pharmacologic properties. Investigative Radiol 1988;23(Suppl 1):S271–4.
[26] Bousquet JC, Saini S, Stark DD, et al. Gd-DOTA: characterization of a new paramagnetic complex. Radiol 1988;166:693–8.
[27] Wedeking P, Tweedle M. Comparison of the biodistribution of ^{153}Gd-labeled $Gd(DTPA)_2$-, Gd(DOTA)-, and $Gd(acetate)_n$ in mice. Int J Rad Appl Instrum Part B. Nucl Med Biol 1988;15:395–402.
[28] Burgess J. Man and the elements of groups 3 and 13. Chem Soc Rev 1996:85–92.
[29] Liu S, Edwards DS. Bifunctional chelators for therapeutic lanthanide radiopharmaceuticals. Biocon Chem 2001;12:7–34.
[30] ten Berge RJ, Natarajan AT, Hardeman MR, van Royen EA, Schellekens PT. Labeling with indium In-111 has detrimental effects on human lymphocytes. J Nucl Med 1983;24:615–20.